J. Fluid Mech. (1986), *vol.* 171, *pp.* 263–287
Printed in Great Britain

Bifurcations of two-dimensional channel flows

By IAN J. SOBEY† AND PHILIP G. DRAZIN
School of Mathematics, University of Bristol, Bristol BS8 1TW, UK

(Received 24 July 1985 and in revised form 16 April 1986)

In this paper we study some instabilities and bifurcations of two-dimensional channel flows. We use analytical, numerical and experimental methods. We start by recapitulating some basic results in linear and nonlinear stability and drawing a connection with bifurcation theory. We then examine Jeffery–Hamel flows and discover new results about the stability of such flows. Next we consider two-dimensional indented channels and their symmetric and asymmetric flows. We demonstrate that the unique symmetric flow which exists at small Reynolds number is not stable at larger Reynolds number, there being a pitchfork bifurcation so that two stable asymmetric steady flows occur. At larger Reynolds number we find as many as eight asymmetric stable steady solutions, and infer the existence of another seven unstable solutions. When the Reynolds number is sufficiently large we find time-periodic solutions and deduce the existence of a Hopf bifurcation. These results show a rich and unexpected structure to solutions of the Navier–Stokes equations at Reynolds numbers of less than a few hundred.

1. Introduction

In this paper we study some instabilities and bifurcations of two-dimensional channel flows. We use all means available, including asymptotic and qualitative analysis as well as numerical and laboratory experiments. It will be seen that the bifurcations of this apparently simple class of flows reveal a rich and unexpected structure of the solutions of the Navier–Stokes equations at not very large values of the Reynolds number. Our calculations show some phenomena not yet observed and for which we have no completely satisfactory explanation. We write much of this paper in the language of bifurcation theory, and thence find new insights into well-known examples such as Jeffery–Hamel flow. This language is appropriate because our interest is in the qualitative nature of channel flows when the parameters which determine the flow are varied. We thereby demonstrate changes in the qualitative nature of the flow, even though we cannot explain why all the changes occur.

Our motivation for this study comes from the well-known observation that flow through a channel which has an expansion throat and is symmetric about its centreline becomes asymmetric as the Reynolds number R increases. This is sometimes called the Coanda effect (cf. Wille & Fernholz 1965), and is explained by observing that an increase in velocity near one wall will lead to a decrease in pressure near that wall and once a pressure difference is established across the channel it will maintain the asymmetry of the flow. There are extensive experimental studies of this phenomenon, for instance by Cherdron, Durst & Whitelaw (1978). The configuration

† Present address: Schlumberger Cambridge Research, P.O. Box 153, Cambridge CB3 0HG, UK.

of the channel may be partially characterized by the expansion ratio D, which is the ratio of the channel width downstream of the expansion to the width upstream. It is convenient to define the Reynolds number of the flow as $R = Q/2\nu$, where Q is the steady volume flux of fluid of kinematic viscosity ν driven along the channel. As R increases from zero the sequence of events is as follows. For sufficiently small values of R a steady symmetric flow is observed. The uniqueness, and therefore symmetry, of this flow is proved by Serrin (1959). For values of R above some critical value a steady asymmetric flow is observed unless D is close to one, in which case a time-periodic flow is observed. The asymmetry can have one of two orientations, according as the main stream is diverted towards one wall of the channel or the other. Thus, for example, in flow through a channel with expansion ratio $D = 3$ asymmetric flows have been observed when $R = 30$. If R is increased further then various events may occur according to the shape of the channel. The flow may remain steady but become three-dimensional. Alternatively, the flow may remain two-dimensional but become time periodic with regular shedding of vortices. Ultimately the flow will, of course, become turbulent as R is increased.

The above description may be translated into the language of bifurcation theory. At sufficiently small values of R there is a unique solution. As R is increased a pitchfork bifurcation occurs and two stable solutions exist. We infer that an unstable solution also exists. Bifurcation theory allows us to clarify the nature of the multiplicity of possible flows, whereas an experiment will give one or other of the stable asymmetric solutions. We can obtain numerically the unstable symmetric solution by imposing suitable boundary conditions, for instance by calculating the flow in one half of the channel. As R is increased further, other bifurcations occur. Thus the steady two-dimensional asymmetric solutions become unstable and a steady three-dimensional flow may occur, indicating other bifurcations. Alternatively a Hopf bifurcation may occur, resulting in a time-periodic solution. Following each bifurcation we can use powerful general theorems to infer the existence of unstable solutions which may be neither observable nor easily calculated.

Some qualitative results of the linear theory are used in § 2 to build a qualitative nonlinear theory of bifurcations of two-dimensional flows. This nonlinear theory is illustrated by the well-known examples of plane parallel flows, swirling flows and Jeffery–Hamel flows. The example of Jeffery–Hamel flow is taken up in detail in § 3, the classical results being presented in a new form suitable for application to two-dimensional flows in two-dimensional channels with walls of small curvature. Important new results about the instability of Jeffery–Hamel flows are presented.

Physical arguments together with all this theory are then used in § 4 as a conceptual basis on which we interpret extensive numerical calculations of some flows in symmetric two-dimensional channels which have a widening followed by a narrowing. The configurations of the channels are illustrated in figure 1. Many bifurcations are identified and elucidated to reveal the rich structure of the regimes of flow as the configuration of the channel and the Reynolds number are varied. The Coanda effect is clearly shown as a break in the symmetry of flow following a pitchfork bifurcation.

These numerical experiments were made in conjunction with laboratory experiments, which are described in § 5. The results of the two kinds of experiment are both supplementary and complementary. The laboratory experiments are in broad agreement with the numerical experiments but not sensitive enough to give the first break of symmetry. The experiments also show that three-dimensional effects, although small at first, become important as the Reynolds number increases.

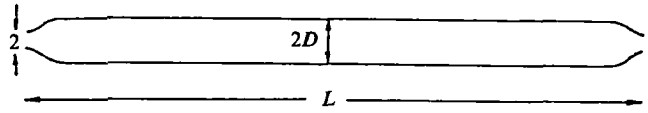

FIGURE 1. A sketch of the configuration of the channels (defined in equation (4.1)).

2. Stability and bifurcation

Let us consider the linear stability of a steady two-dimensional flow of a viscous incompressible fluid. We denote the basic velocity of the fluid by $\boldsymbol{U}(x, z, R)$, where we use dimensionless variables based on some length- and velocity-scales, and where R is the corresponding Reynolds number. For channel flows, we shall adopt the convention that the dimensionless volume flux is two. We let V be the domain of the flow in the (x, z)-plane and specify the flow by appropriate conditions on the boundary ∂V of the domain. These conditions may be that $\boldsymbol{U}$ is given on some parts and is periodic on other parts of ∂V.

To examine the stability of this basic flow, let the velocity of the perturbed flow be

$$\boldsymbol{u}(\boldsymbol{x}, t) = \boldsymbol{U}(x, z, R) + \epsilon \boldsymbol{u}'(\boldsymbol{x}, t, R), \tag{2.1}$$

for a small parameter ϵ, and linearize the Navier–Stokes equations as $\epsilon \to 0$ for fixed $R = Q/2\nu$. Therefore

$$\boldsymbol{u}'_t + \boldsymbol{U}\cdot\boldsymbol{u}' + \boldsymbol{u}'\cdot\nabla\boldsymbol{U} = -\nabla p' + R^{-1}\nabla^2\boldsymbol{u}' \tag{2.2}$$

and

$$\nabla\cdot\boldsymbol{u}' = 0 \quad \text{in } V, \tag{2.3}$$

where $\epsilon p'$ is the dimensionless perturbation of the pressure. In the usual way, we use the method of normal modes to solve the linearized problem, taking

$$\boldsymbol{u}'(\boldsymbol{x}, t) = \mathrm{Re}\,[\mathrm{e}^{st}\hat{\boldsymbol{u}}(\boldsymbol{x})], \quad p'(\boldsymbol{x}, t) = \mathrm{Re}\,[\mathrm{e}^{st}\hat{p}(\boldsymbol{x})], \tag{2.4}$$

for an eigenvalue s and eigenvector $(\hat{\boldsymbol{u}}, \hat{p})$ to be determined. Therefore

$$s\hat{\boldsymbol{u}} + \boldsymbol{U}\cdot\nabla\hat{\boldsymbol{u}} + \hat{\boldsymbol{u}}\cdot\nabla\boldsymbol{U} = -\nabla\hat{p} + R^{-1}\nabla^2\hat{\boldsymbol{u}}, \tag{2.5}$$

and

$$\nabla\cdot\hat{\boldsymbol{u}} = 0 \quad \text{in } V. \tag{2.6}$$

There will also be appropriate linear homogeneous boundary conditions on ∂V.

For two-dimensional disturbances, the problem may be simplified a little by taking the stream function Ψ of the basic flow and $\hat{\psi}$ of the disturbance so that

$$\boldsymbol{U} = (\Psi_z, 0, -\Psi_x), \quad \boldsymbol{u}' = \mathrm{Re}\,[\mathrm{e}^{st}(\hat{\psi}_z, 0, -\hat{\psi}_x)]. \tag{2.7}$$

Then the Navier–Stokes equations reduce to the linearized vorticity equation,

$$s\nabla^2\hat{\psi} + \Psi_z\nabla^2\hat{\psi}_x - \Psi_x\nabla^2\hat{\psi}_z + (\nabla^2\Psi_x)\hat{\psi}_z - (\nabla^2\hat{\psi}_z)\hat{\psi}_x = R^{-1}\nabla^4\hat{\psi} \quad \text{in } V. \tag{2.8}$$

There will also be linear homogeneous conditions on ∂V, so that, for example, $\hat{\psi} = \partial\hat{\psi}/\partial n = 0$ on some parts of ∂V and $\hat{\psi}$ and $\partial\hat{\psi}/\partial n$ are periodic on the other parts. Equation (2.8) is of the form

$$q\nabla^2\hat{\psi} - R\mathrm{M}\hat{\psi} = \nabla^4\hat{\psi}, \tag{2.9}$$

where $q = Rs$ and M is a linear differential operator which depends on Ψ but does not depend explicitly on R.

This poses a real eigenvalue problem, so that for given Ψ and R, each eigenvalue q is either real or one of a complex conjugate pair. When V is bounded the eigen-

values are discrete and in general simple; then they may be ordered so that $\mathrm{Re}\, q_1 \geqslant \mathrm{Re}\, q_2 \geqslant \ldots$.

When $R = 0$ the problem in (2.9) is formally symmetric. Therefore the eigenvalues, $q_n^{(0)}$ say, are all real, and we may order them so that $q_1^{(0)} > q_2^{(0)} > \ldots$. Further the flow is stable, with $0 > q_1^{(0)}$, if R is chosen so that the limit $R \to 0^+$ corresponds to the dimensional flow tending to zero everywhere and thence to Stokes flow (Serrin 1959, p. 254). It should be remembered that in general Ψ involves R and that it may be desirable to choose R in such a way that Stokes flow is not the only flow to arise when $R = 0$.

As R increases from zero the eigenvalues q_n all remain real until two coincide and become a complex conjugate pair. This may occur before or after the onset of instability, i.e. before or after R reaches the value R_c for which $\mathrm{Re}\, q_1 = 0$. If it occurs before then we have $\mathrm{Im}\, q_1 \neq 0$ at $R = R_c$, and if afterwards then $\mathrm{Im}\, q_1 = 0$ at $R = R_c$. In the latter case some authors say that the principle of the exchange of stabilities is valid. It is also possible that the eigenvalues may remain real for all values of R.

The solutions q of a quadratic equation whose real coefficients depend upon R offer a simple illustration of the functional analytic background to the previous paragraph. Davis (1969) discussed this issue of hydrodynamic stability in quite general terms, although his results are not strictly applicable to the present problem. DiPrima & Hall (1984) have shown, in an interesting example of axisymmetric instability of Couette flow between two cylinders, that two higher modes coalesce and become complex although the most unstable mode remains real as the Reynolds number increases.

Squire's transformation governs the stability of plane parallel basic flows, so some flows are most unstable to two-dimensional disturbances. However, axisymmetric disturbances are often the most unstable for Couette flow between rotating cylinders, so that two-dimensional disturbances are not the most unstable for *all* two-dimensional basic flows.

If the basic flow, $\boldsymbol{U} = (U, 0, W)$, is symmetric about some centreline, say $z = 0$, then $U(x, -z) = U(x, z)$ and $W(x, -z) = -W(x, z)$. It follows that each eigenmode is either antisymmetric or symmetric, i.e. $\hat{\psi}_n$ is either an even or odd function of z respectively. Now when $R = 0$ the eigenvalue problem is real and self-adjoint and so may be formulated as a variational principle, which shows that the least stable mode has an antisymmetric eigenfunction $\hat{\psi}_1$. By continuity, the reality and ordering of the antisymmetric and symmetric eigenfunctions for a symmetric basic flow will persist as R increases from zero until two eigenvalues coalesce. The coalescence of the eigenvalues of symmetric flows is as follows. If two real eigenvalues coalesce and become complex as R increases then both eigenfunctions remain either antisymmetric or symmetric; if two real eigenvalues coalesce and remain real as R increases then the eigenfunctions may be antisymmetric or symmetric but their symmetry will be unaltered by the coalescence.

By appeal to quite general results of bifurcation theory, much can be revealed about the qualitative nature of the bifurcation of steady flows. We summarize here the results we need to use later. Justification of these results and more details are given by, for example, Benjamin (1978) and Drazin & Reid (1981). We will then go on to illustrate the summary with a few examples of two-dimensional flows.

For bounded flows, the most unstable normal mode is unique or one of a complex conjugate pair, and the linear theory of stability gives the stream function in the former case as

$$\psi(x, z, t) = \Psi(z) + \epsilon A(t)\, \hat{\psi}_1(x, z) + \text{smaller terms}. \tag{2.10}$$

as $\epsilon \to 0$ for each value of R, where $A(t) = A_0 \exp(s_1 t)$ and $s_1 \sim k(R - R_c)$ as $R \to R_c$ for some $k > 0$. The weakly nonlinear theory gives a similar result when R is close to R_c, although A satisfies a nonlinear evolution equation such as the Landau equation of the form

$$\frac{dA}{dt} = s_1 A - l|A|^2 A, \tag{2.11}$$

and therefore does not grow exponentially with time.

As R increases, the number and character of the steady solutions may change. It is often convenient to take some functional, ζ say, of the infinite-dimensional space of solutions of the Navier–Stokes equations so that each steady solution $\boldsymbol{u}, p$ is represented by the single quantity ζ. Thereby we may plot the steady solutions as a function of R in a plane bifurcation diagram which is the graph of ζ as a function of R. To represent the infinite-dimensional solution a little better it may be useful to take two or more state variables like ζ. The aim is to choose variables that are both physically informative and also easy to calculate or measure. Often one component of the velocity at a suitable given point of the flow is a good state variable to use.

A typical transition from a stable to an unstable steady flow, when a simple real eigenvalue of a mode increases through zero as R increases through a critical value, is a turning point. Also transcritical and pitchfork bifurcations of steady flows are common, the latter being associated with the breaking of some symmetry of flow. Except at values of R where bifurcations occur, the number k of steady flows is odd and at least $\frac{1}{2}(k-1)$ of them are unstable (Benjamin 1978). It follows that there is at least one symmetric steady flow when the configuration is symmetric. Hopf bifurcations, at which steady flows become time periodic, are also common. Again, other bifurcations occur along the route to turbulence, but we shall not meet them here.

In interpreting laboratory and numerical results it is important to remember that they are imperfect, i.e. that they have small discrepancies from their ideals and, in particular, may be only approximately symmetric. Of the elementary bifurcations we have mentioned, only a turning point and a Hopf bifurcation are unaltered by small imperfections.

Plane parallel flows are an important class of two-dimensional flows. Plane Couette flow is stable to all infinitesimal disturbances, whatever the value of the Reynolds number, but unstable to disturbances of finite amplitude at sufficiently large values of the Reynolds number. The nature of other flows compatible with the boundary conditions of plane Couette flow is poorly understood. Plane Poiseuille flow, with velocity distribution $U(z) = \frac{3}{2}(1-z^2)$, say, is stable to infinitesimal disturbances for $R < R_c$, where $R_c \approx 3848$, and unstable for $R > R_c$. (Remember that we have chosen the scales so that the dimensionless volume flux of the flow is two.) By Squire's transformation, the most unstable mode at the onset of instability is two-dimensional. It is, however, only the most unstable of a continuum of three-dimensional modes. The nonlinear theory gives a subcritical Hopf bifurcation at $R = R_c$ and a complicated set of three-dimensional unsteady flows.

Jeffery–Hamel flows are another well-known example. These two-dimensional steady flows in converging and diverging channels with plane walls are described in many textbooks. The rich structure of their bifurcations has been elucidated recently by Fraenkel (1962) and Buitrago (1983), though the structure is not widely understood because of the complication of dependence of the solutions on the parameters in which it is most convenient *mathematically* to describe the flows. There

is little to add to Fraenkel's (1962) account of the steady Jeffery–Hamel flows themselves, but in §3 we shall recalculate some of his solutions in a form which is more useful physically, identify a pitchfork bifurcation, and justify the important result that most of the types of Jeffery–Hamel solutions are unstable.

The flow in a channel may be described by the use of various approximations. To be specific, let the walls of the channel have equations $z = f(x), z = -g(x)$, where the x-axis is directed along the channel. Then the domain of the flow is $-g(x) \leqslant z \leqslant f(x)$. Also the tangents to the walls at each station x make angles $\alpha(x) = \tan^{-1} \mathrm{d}f/\mathrm{d}x$ and $\beta(x) = \tan^{-1} \mathrm{d}g/\mathrm{d}x$ with the x-axis.

If $\alpha, \beta \ll 1$ then the flow is quasi-parallel and a plane parallel flow is a local approximation to the flow along the channel. This approximation was used by Eagles (1966) to examine the instability of a family of Jeffery–Hamel flows in a divergent channel. He was led to solve the Orr–Sommerfeld equation to find the instability. This approximation, essentially that the width of the channel varies slowly downstream, has been developed and applied by Eagles & Weissman (1975) and Eagles & Smith (1980).

If $\mathrm{d}\alpha/\mathrm{d}x, \mathrm{d}\beta/\mathrm{d}x \ll 1$ then the angles of the walls change slowly, i.e. their curvature is small, and a Jeffery–Hamel flow is plausibly a local approximation to flow along a channel. This approximation was used by Fraenkel (1962, 1963) to describe some steady flows in channels, and will be developed in §§3 and 6. Fraenkel described in detail only steady symmetric flows in symmetric channels. Georgiou & Eagles (1985) examined the linear stability of such flows when the curvature of the channel walls is small.

These asymptotic methods are useful for many flows, but for many others there is local instability and a breakdown, so that the flows are mostly not quasi-parallel or nearly Jeffery–Hamel. It should be recognized that each flow is steady or time-periodic as a whole, and each flow becomes unstable as a whole. Also local instability of small but finite amplitude may lead to a breakdown of the assumed basic flow. Nonetheless, the approximations of parallel flow and of small wall curvature are valuable in the interpretation of the evolution of disturbances and the development downstream of real flows. For example, a flow may be stable, yet small initial disturbances may grow where the flow is locally unstable, propagate downstream, and finally decay where the flow is locally stable. So it is desirable to use asymptotic results as well as experiments, numerical calculations, physical mechanisms and qualitative theory.

3. Jeffery–Hamel flows

Jeffery (1915) and Hamel (1916) independently considered the steady radial flow of a viscous incompressible fluid between two inclined plane walls. They found a similarity transformation to reduce the Navier–Stokes equations to an ordinary differential equation, and derived some interesting results. Their work was developed by many authors, an essentially complete solution being given by Fraenkel (1962). However, Buitrago (1983) has recently given more details of the asymmetric solutions, and Hooper, Duffy & Moffatt (1982) applied the transformation to flows of a fluid of variable viscosity. In this section, we shall first recapitulate the Jeffery–Hamel (called JH hereinafter) problem, then recalculate some results in a new form suited to our study of the instability and bifurcation of channel flows and finally investigate the instability of JH flows.

Let (r, θ) be plane polar coordinates so that the equation of the walls are $\theta = \pm\alpha$

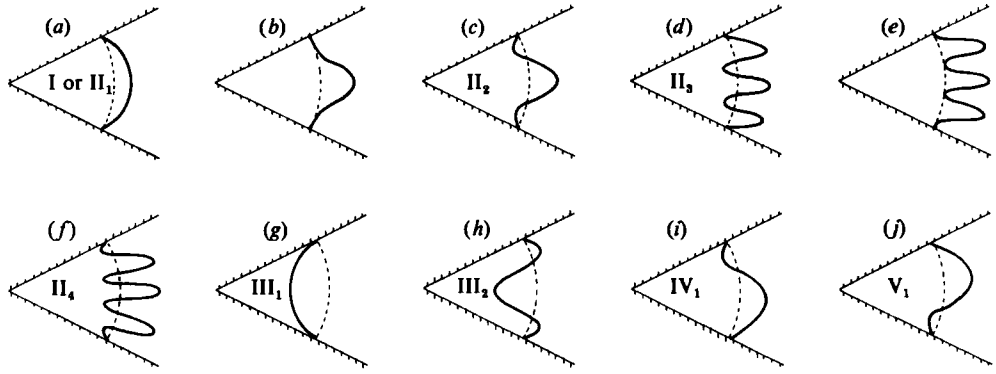

FIGURE 2. Sketches of velocity profiles of some Jeffery–Hamel flows. (*a*) Type I or II_1. (*b*) Type II_1, II_2, IV_1 or V_1 at bifurcation $\mathscr{R}_2$. (*c*) Type II_2. (*d*) Type II_3. (*e*) Type II_3, II_4, IV_2, V_2 at bifurcation. (*f*) Type II_4. (*g*) Type III_1. (*h*) Type III_2. (*i*) Type IV_1. (*j*) Type V_1. The sketches indicate the velocity profile, and therefore the function $g(y)$, as θ increases from $-\alpha$ at the lower wall to α at the upper wall for a fixed value of r.

and that $r > 0$ and $-|\alpha| < \theta < |\alpha|$ in the domain of flow. We assume that the flow is everywhere in the radial direction due to a line singularity at $r = 0$, and has velocity u, say. Then the stream function Ψ is a function of θ alone, $u = r^{-1}\,\mathrm{d}\Psi/\mathrm{d}\theta$, and the volumetric flux between the walls is given by $Q = \int_{-\alpha}^{\alpha} ur\,\mathrm{d}\theta$. By convention, we take $Q \geqslant 0$, so that $\alpha < 0$ for flow converging to a sink at $r = 0$, and define $R = Q/2\nu$, where ν is the kinematic viscosity of the fluid. Then R may be small, or even zero, when the maximum velocity of the flow is large. On defining $y = \theta/\alpha$ and $G(y) = 2\Psi(\theta)/Q$, the Navier–Stokes equations reduce to the ordinary differential equation

$$G_{yyyy} + 4\alpha^2 G_{yy} + 2\alpha R G_y G_{yy} = 0, \tag{3.1}$$

governed by the boundary conditions,

$$G = \pm 1, \quad G_y = 0 \quad \text{at } y = \pm 1 \text{ respectively.} \tag{3.2}$$

It is also convenient to define $g = G_y$, so that $u = Qg/2\alpha r$.

There are five types, I–V, of JH solutions (cf. Fraenkel 1962). For types I and II_1 there is a symmetric pure outflow, i.e. $u(r, -\theta) = u(r, \theta)$ and $u(r, \theta) > 0$ for $-\alpha < \theta < \alpha$. For type II_n there is a symmetric net outflow, u having $2n-2$ zeros between the walls, for $n = 1, 2, \ldots$. For type III_n there is symmetric net inflow, u having $2n-2$ zeros between the walls. Thus for type III_1 there is a symmetric pure inflow. For types IV_n and V_n there is asymmetric flow, with outflow and inflow as θ varies. For type IV_n there is outflow near the wall $\theta = -\alpha$, and u has $2n-1$ zeros between the walls. Each flow of type V_n is the mirror image in the centreline $\theta = 0$ of a flow of type IV_n, and vice versa. These types of flow are illustrated in figure 2. All solutions may be specified in terms of Jacobian elliptic functions.

For the record, note that Buitrago (1983, p. 10) inferred from Fraenkel's (1962) paper the details of solutions of type IV_n, stating explicitly that

$$\alpha = nQ^{\frac{1}{2}}K(m), \quad R = 6nQ^{-\frac{1}{2}}\{E(m) - K(m)\,\mathrm{dn}^2(\beta|m)\}, \tag{3.3}$$

and

$$g(y) = 6mnK(m)\,Q^{-\frac{1}{2}}R^{-1}\{\mathrm{sn}^2(\beta|m) - \mathrm{sn}^2(nK(m)\,(y+1) - \beta|m)\}, \tag{3.4}$$

for $0 \leqslant m \leqslant 1$ and $0 \leqslant \beta \leqslant K(m)$, where $Q = 1 + m - 3m\,\mathrm{sn}^2(\beta|m)$. The explicit solutions V_n follow by symmetry in $\pm y$.

m	0	0.05	0.1	0.15	0.2	0.25
α	$\frac{1}{2}\pi$	1.50936	1.44221	1.36815	1.28554	1.19201
R	0	0.24995	0.53371	0.86167	1.24970	1.72378
m	0.3	0.35	0.4	0.42	0.44	0.45
α	1.08396	0.95542	0.79493	0.71666	0.62573	0.57360
R	2.33035	3.16434	4.46606	5.26089	6.38634	7.16760
m	0.46	0.47	0.475	0.48	0.485	0.49
α	0.51522	0.44812	0.40997	0.36750	0.31897	0.26102
R	8.20642	9.69954	10.74817	12.15448	14.19409	17.57969
m	0.492	0.494	0.496	0.498	0.5	
α	0.23367	0.20255	0.16553	0.11715	0	
R	19.74228	22.89765	28.16787	40.01103	∞	

TABLE 1. The boundary $\mathscr{B}_2$, with equation $\alpha = \alpha_2(R)$ in the (α, R)-plane, which marks the onset of instability of JH solutions of type II_1 and the bifurcation of types II_1, II_2, IV_1 and V_1. The boundary is given in terms of the parameter m by $\alpha = (1-2m)^{\frac{1}{2}}K(m)$ and $R = 6(1-2m)^{-\frac{1}{2}}\{E(m)-(1-m)K(m)\}$ for $0 \leqslant m < \frac{1}{2}$ in the notation of Fraenkel (1962), where K and E are the complete elliptic integrals. Note that $\alpha \sim (1-2m)^{\frac{1}{2}}K(\frac{1}{2})$ and $R \sim 6(1-2m)^{-\frac{1}{2}} \times \{E(\frac{1}{2})-\frac{1}{2}K(\frac{1}{2})\}$ as $m \uparrow \frac{1}{2}$ so that $\alpha \sim 4.712/R$ as $R \to \infty$.

For each pair of values of α and R, many solutions occur, as is recounted by Fraenkel (1962), Hooper *et al.* (1982) and Buitrago (1983). Some curves of transition from one type of solution to another are shown in figure 5 of Fraenkel (1962). We also give in table 1 some recalculations of the important boundary $\mathscr{B}_2$, which marks the pitchfork bifurcation where flows of types II_1, II_2, IV_1 and V_1 coincide. Figure 2(*b*) is a sketch of the velocity profile of the flow at the bifurcation.

Bifurcation diagrams in the planes of $g(0)$ and α, and of $g'(0)$ and α, for $R = 20$ are given in figure 3. The diagrams show how multiple equilibria arise as α passes its values on boundaries such as $\mathscr{B}_2$. Note that $g(0)$ is proportional to the velocity and $g'(0)$ to the transverse velocity gradient on the centreline $\theta = 0$, and that we take $\alpha > 0$ for net outflow and $\alpha < 0$ for net inflow. We have chosen $R = 20$ as a useful and 'typical' value, the qualitative characters of the bifurcation diagrams for $\alpha < \frac{1}{2}\pi$ being similar for all R, although Buitrago (1983) demonstrates that there are cusps on the boundaries $\mathscr{B}_n$ for $\alpha > \frac{1}{2}\pi$. As R increases more solutions occur in the range $-\frac{1}{2}\pi < \alpha < \frac{1}{2}\pi$ relevant to channel flows. Note, in particular, that as α increases through its value $\alpha_3(R)$ on $\mathscr{B}_3$ the JH flows of type II_2 are not succeeded continuously by any JH flow, as is evident in the work of Fraenkel (1962) and of Moffatt & Duffy (1980, § 5), who considered the case $R = 0$ and denoted α_3 by α_c.

To investigate the stability of these flows, we may use the ideas of § 2. The solutions of types I and III_1 must be stable for sufficiently small values of R, because the maximum velocity of the flow (at least if we exclude a neighbourhood of $r = 0$ from the domain of the flow) may be made as small as we please. Also, as $\alpha \to 0$ for fixed R, the flow tends to plane Poiseuille flow, and therefore is stable if $R < 3848$. Therefore, by continuity, it is plausible that the flows III_1, I and II_1 remain stable as α decreases or increases from zero. Examination of the bifurcation at $\mathscr{B}_2$ shows that it is a subcritical pitchfork. Therefore the solution II_2 becomes unstable to an antisymmetric mode as α increases beyond its critical value $\alpha_2(R)$ on $\mathscr{B}_2$, II_1 being stable subcritically, II_2 unstable supercritically, and IV_1 and V_1 unstable subcritically. It is possible, however, that flows III_1, I or II_1 may become unstable first to a two-dimensional disturbance incompatible with the similarity form of the JH flows

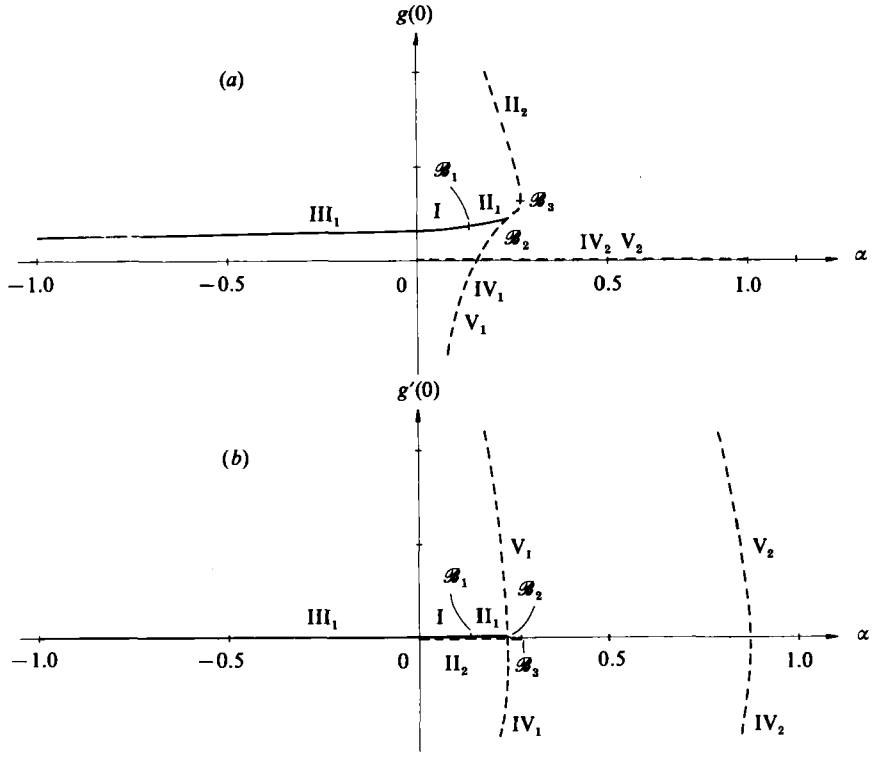

FIGURE 3. The bifurcation diagram of some Jeffery–Hamel flows for $R = 20$ in (a) the $(\alpha, g(0))$-plane and (b) the $(\alpha, g'(0))$-plane. Note that the subcritical pitchfork bifurcation $\mathscr{P}_2$ is seen in two projections in these planes.

or, indeed, to a three-dimensional disturbance. As we shall see, the latter possibility is implausible in the light of laboratory experiments. When α increases to its value on $\mathscr{P}_3$ the solution II_2 has a turning point and becomes unstable to a second mode, which is symmetric.

These results may be substantiated by numerical solution of the eigenvalue problem of § 2. Rather than face this formidable problem, we take a model problem after Hooper *et al.* (1982, p. 303), namely

$$G_{yyt} = G_{yyyy} + 4\alpha^2 G_{yy} + 2\alpha R G_y G_{yy}, \tag{3.5}$$

and

$$G = \pm 1, \quad G_y = 0 \quad \text{at } y = \pm 1 \text{ respectively.} \tag{3.6}$$

The system (3.5) and (3.6) reduces to the JH problem (3.1) and (3.2) for steady solutions, $\overline{G}$ say, and also represents the convection and diffusion of vorticity by the use of the time derivative on the left-hand side of equation (3.5). To consider the 'stability' of a JH flow then, put

$$G(y,t) = \overline{G}(y) + \epsilon G'(y,t), \tag{3.7}$$

linearize equation (3.5) for small ϵ, and take normal modes of the form

$$G'(y,t) = \mathrm{Re}\{e^{st} G_1(y)\}.$$

It follows that

$$s\frac{d^2G_1}{dy^2} = \frac{d^4G_1}{dy^4} + 4\alpha^2\frac{d^2G_1}{dy^2} + 2\alpha R\left(\frac{d\overline{G}}{dy}\frac{d^2G_1}{dy^2} + \frac{d^2\overline{G}}{dy^2}\frac{dG_1}{dy}\right), \tag{3.8}$$

and
$$G_1 = \frac{\mathrm{d}G_1}{\mathrm{d}y} = 0 \quad \text{at } y = \pm 1. \tag{3.9}$$

Multiplication of equation (3.8) by the complex conjugate G_1^* of G_1 and integration from $y = -1$ to 1 then gives the 'energy' equation,

$$-s\int_{-1}^{1}\left|\frac{\mathrm{d}G_1}{\mathrm{d}y}\right|^2\mathrm{d}y = \int_{-1}^{1}\left(\left|\frac{\mathrm{d}^2G_1}{\mathrm{d}y^2}\right|^2 - 4\alpha^2\left|\frac{\mathrm{d}G_1}{\mathrm{d}y}\right|^2 - 2\alpha R\frac{\mathrm{d}\overline{G}}{\mathrm{d}y}\left|\frac{\mathrm{d}G_1}{\mathrm{d}y}\right|^2\right)\mathrm{d}y, \tag{3.10}$$

on integration by parts and the use of boundary conditions (3.9). Therefore s, and thence G_1, is real. Indeed we see that the eigenvalue problem, (3.8) and (3.9), is real and self-adjoint; also (3.8) may be deduced from a variational principle, corresponding to a minimum of the 'energy', in which s arises as an undetermined multiplier.

The JH flows of types I, II_n and III_n are symmetric and therefore $\overline{G}$ is an odd function of y. Therefore the eigenvalue problem, (3.8) and (3.9), is symmetric, and each eigenfunction G_1 is either an odd or an even function of y, corresponding respectively to a symmetric or an antisymmetric disturbance of the JH flow. The variational principle shows that the eigenfunction G_1 of the least stable mode is even.

An integral of equation (3.8) is

$$\frac{\mathrm{d}^2g_1}{\mathrm{d}y^2} + \left(4\alpha^2 + 2\alpha R\frac{\mathrm{d}\overline{G}}{\mathrm{d}y} - s\right)g_1 = \text{constant},$$

where we define $g_1 = \mathrm{d}G_1/\mathrm{d}y$. If G_1 is even, then g_1 is odd and the constant is zero. Therefore the most unstable mode is governed by the Sturm–Liouville problem

$$\frac{\mathrm{d}^2g_1}{\mathrm{d}y^2} + \left(4\alpha^2 + 2\alpha R\frac{\mathrm{d}\overline{G}}{\mathrm{d}y} - s\right)g_1 = 0, \tag{3.11}$$

and
$$g_1 = 0 \quad \text{at} \quad y = 0, 1. \tag{3.12}$$

Equation (3.1) implies that when $s = 0$ a solution of (3.11) is given by $g_1 = \mathrm{d}^2\overline{G}/\mathrm{d}y^2$. This also satisfies the boundary conditions (3.12) when $\alpha = \alpha_2(R)$ on $\mathscr{B}_2$, because then $\mathrm{d}^2\overline{G}/\mathrm{d}y^2$ vanishes on the boundaries $y = \pm 1$, as is illustrated in figure 2 (*b*). Thus we have a simple expression, in terms of Jacobian elliptic functions, for the eigenfunction at the margin of stability. This is true not only for the model problem but also for the proper problem (2.8) when $s = 0$.

We have solved the problem (3.1) and (3.2) near the bifurcation on $\mathscr{B}_2$ by the use of weakly nonlinear theory. The solution may be sketched as follows. The essential idea is to perturb the explicitly known solution of the linear problem at marginal stability. Accordingly, we define $\epsilon = |\alpha - \alpha_2|^{\frac{1}{2}}$, let $\alpha = \alpha_2 + \epsilon^2\alpha''$ for $\alpha'' = \pm 1$, define the slow timescales $t_n = \epsilon^n t$ for $n = 2, 3, \ldots$, and make the formal expansions

$$G(y, t, \alpha, R) = \overline{G}(y, R) + \epsilon G'(y, t, R) + \epsilon^2 G''(y, t, R) + \ldots, \tag{3.13}$$

$$\frac{\partial}{\partial t} = \epsilon^2\frac{\partial}{\partial t_2} + \epsilon^3\frac{\partial}{\partial t_3} + \ldots \quad \text{as} \quad \epsilon \to 0. \tag{3.14}$$

The expansions are justified heuristically in the sense that we have iterated the solution and found consistent solutions for G' and G'' in turn (cf. Drazin & Reid 1981, § 56). The technical success of the method depended on our being able to find a Green function to invert the ordinary differential operator,

$$\mathrm{L} = \frac{\mathrm{d}^4}{\mathrm{d}y^4} + 4\alpha_2^2\frac{\mathrm{d}^2}{\mathrm{d}y^2} + 2\alpha_2 R\left(\frac{\mathrm{d}\overline{G}}{\mathrm{d}y}\frac{\mathrm{d}^2}{\mathrm{d}y^2} + \frac{\mathrm{d}^2\overline{G}}{\mathrm{d}y^2}\frac{\mathrm{d}}{\mathrm{d}y}\right), \tag{3.15}$$

associated with the linear stability equation (3.8) and boundary conditions (3.9) for $\epsilon = 0$. It follows that

$$G'(y, t, R) = A(t_2, R)\frac{\mathrm{d}\overline{G}}{\mathrm{d}y}(y, R), \tag{3.16}$$

where A satisfies an amplitude evolution equation of the form

$$\frac{\mathrm{d}A}{\mathrm{d}t_2} = \frac{\alpha-\alpha_2}{|\alpha-\alpha_2|}kA - lA^3 \quad \text{as } \epsilon \to 0. \tag{3.17}$$

The constants k and l are complicated, being ratios of explicit integrals of algebraic functions of $\mathrm{d}\overline{G}/\mathrm{d}y$ and $\mathrm{d}^2\overline{G}/\mathrm{d}y^2$, such that $k > 0$ and $l < 0$. This gives the subcritical pitchfork bifurcation, with $A = 0$ for the steady JH flows of types II_1 and II_2 near bifurcation, and $A = \pm(k/(-l))^{\frac{1}{2}}$ for flows of types IV_1 and V_1 when $\alpha < \alpha_2$.

Direct numerical solution of the linear stability problem (3.11) and (3.12) gives the onset of instability at $\alpha = 0.2308$ with $k = 41.5$ for $R = 20$.

We envisage that a similar method may be applied to the nonlinear vorticity equation to give the proper weakly nonlinear solution and show that there is a subcritical pitchfork bifurcation described by another amplitude equation of the form (3.17). The technical feasibility of such a method would depend upon using a Green function to invert the partial differential operator associated with the linear stability equation (2.8) for $\epsilon = 0$.

The subcritical pitchfork bifurcation of the JH solutions on $\mathscr{B}_2$ casts some light on the flow through slowly varying channels. Fraenkel (1973) proved that there exists a flow through a slowly varying symmetric channel which is approximated locally by a symmetric JH flow for $\alpha < \alpha_3(R)$. We now see that this may occur where $\alpha < \alpha_2(R)$ for the value of R characterizing the steady flux along the channel, but that for $\alpha_2(R) < \alpha < \alpha_3(R)$ the flow is locally unstable and for $\alpha > \alpha_3(R)$ there is no contiguous symmetric JH flow to which the channel flow could develop continuously. It is therefore plausible that Fraenkel's result is relevant in practice only if $\alpha < \alpha_2(R)$ everywhere along the channel.

This instability of JH flows may be related to the quasi-parallel theory of Eagles (1966, 1973) for large values of the Reynolds number. However that theory is relevant to channel flow only when the angles between the tangents to the walls of the channel and a centreline are small, and so the flow approaches plane Poiseuille flow, because otherwise the flow will be unstable and break down. We have shown that the instability of a JH flow of type II_1 as α increases above $\alpha_2(R)$ is the important one and that the marginally stable mode is stationary. This contrasts with Eagles' finding complex eigenvalues for the most unstable modes which would seem, as in plane Poiseuille flow, to lead to a Hopf bifurcation, not a pitchfork bifurcation. Eagles also found some less unstable modes with phase velocities in the opposite direction to the basic flow, as Drazin (1961) had found earlier for a two-dimensional jet; so there is a stationary mode in these examples, but it is not the most unstable mode. These 'unexpected' results may be the vestige, in the quasi-parallel approximation, of the fact that the most unstable mode of the 'exact' divergent flow is stationary and that the 'real' bifurcation is a pitchfork.

4. Calculations of solutions for channel flows

In this section we review a large number of numerical experiments of two-dimensional flow in a symmetric channel. The calculations were undertaken to

simulate laboratory experiments which show asymmetric flow through a symmetric channel. The configuration used most frequently in experiments is a backward-facing step (cf. Cherdron *et al.* 1978) in which a parallel channel undergoes a sudden symmetric expansion to become another parallel channel. Our numerical methods cannot deal adequately with a sudden expansion so we have smoothed the expansion. Because we cannot simulate an infinite length of channel and we wish to avoid the introduction of approximate solutions at the up- and downstream ends of the channel, we have assumed that the channel is periodic in the longitudinal direction. Given these limitations, the calculations agree well with the known experimental work and, furthermore, predict some phenomena which have not yet been observed.

Since the details of our numerical method are important in discussion of the calculated flows, we start by describing the method. It was developed by Gillani & Swanson (1976) for flow through a cylindrical channel, and we have adapted it for two-dimensional flows. The method has been used successfully for years (cf. Sobey 1980, 1982). The solution proceeds by assuming that the stream function ψ and the vorticity field ω are known at a given time, t say, and then integrating the vorticity equation to calculate the vorticity at a later time, $t+\delta t$ say, in the interior of the channel. A Poisson equation is then solved to obtain the stream function at the later time and the values of the stream function give the vorticity on the walls of the channel. The cycle is now complete, and the fields at time $t+2\delta t$ can be calculated, and so forth. This basic method is modified in two ways. Firstly, by a Dufort–Frankel substitution, the vorticity fields at *two* previous time steps, $t-\delta t$ and t, are used. Secondly, the nonlinear terms are upwind differenced so that the sign of the velocity determines the representation of derivatives such as $\partial(u\omega)/\partial x$. At each grid point the velocities are tested for $u > 0$, $u = 0$, or $u < 0$, and a different scheme used in each case. Full details are given by Gillani & Swanson. In our particular problem several further details are relevant. Specifying the channel boundary by $z = \pm f(x)$, we define a new lateral coordinate $y = z/f(x)$ and transform the problem to the (x, y)-plane. If we define L as the period of the channel in the x-direction, the domain of the flow becomes the rectangle $0 \leqslant x \leqslant L$ and $-1 \leqslant y \leqslant 1$. The transformation also introduces terms which involve $\partial^2/\partial x\,\partial y$, and therefore a nine-point finite-difference scheme is used. A new nonlinear term $\partial(u\omega)/\partial y$ arises. We have upwinded this term, using the sign of u but ignoring the sign of v. The only other non-standard device we have used is to apply the Dufort–Frankel substitution to the nonlinear terms in addition to the viscous terms. So, for differences at the ijth node, $\omega_{ij}(t)$ is replaced by $\frac{1}{2}\{\omega_{ij}(t+\delta t)+\omega_{ij}(t-\delta t)\}$ throughout the entire scheme. At the boundaries we calculate the wall vorticity by a simple two-point formula. We also used Woods' (1954) method but the results were little affected and we reverted to the simpler method for all the calculations described below. When solving the Poisson equation for the stream function we used over-relaxation and iterated the solution until the upstream and downstream boundaries were matched. Following Gillani & Swanson, we used composite grids, with a fine grid near the channel walls and a coarse grid near the centre of the channel. For the case $L = 80$, there were 962×5 grid points near each wall and 242×19 in the centre of the channel, giving 14218 points distributed through the channel; for the case when $L = 40$ the number of points was halved.

The accuracy of the numerical scheme is first order in the grid size and second order in the time step. The calculations are, of course, not perfect, and imperfect bifurcations occur instead of perfect bifurcations. Also the scheme introduces the well-known phenomenon of artificial viscosity, so there is an upper bound on the values of R for which the accuracy is acceptable. Comparison of the results of our

numerical and laboratory experiments suggests that the numerical results are good for values of R up to about 150. Thus the numerical solutions are very accurate approximations to the well-defined nonlinear finite-difference equations, which we believe represent faithfully the behaviour of Newtonian fluids for a wide range of values of the Reynolds number. This belief is ultimately based on comparison of laboratory and numerical experiments.

We are primarily interested in steady solutions, but we calculate them by solving initial-value problems. We assume that the flow is accelerated from rest during a short period and is then left to become steady. The Dufort–Frankel substitution requires the field at two time steps. We take $\omega = \psi = 0$ throughout the channel at $t = 0$. We assumed that during the first time step the motion is inviscid, and solved $\nabla^2\psi = 0$ to find the stream function associated with the small flux at time δt. Then, knowing the stream function, we calculated the wall vorticity by assuming that the vorticity had diffused no further than $(\nu\delta t)^{\frac{1}{2}}$ during the first timestep. Throughout the interior of the channel the vorticity was set to zero. In this way the solution could be calculated from $2\delta t$ onwards until a steady solution emerges after some time.

Note that numerical methods are very powerful for the study of these flows because we can calculate the unstable symmetric solutions as well as the stable asymmetric solutions. Some symmetric solutions unstable to antisymmetric disturbances are calculated by setting $\psi = 0$ on the centreline of the channel and by integrating the solution in only one half of the channel.

The configuration of the channel is defined by its equation $z = \pm f(x)$ where

$$f(x) = \begin{cases} 1+\frac{1}{2}(D-1)\{1-\cos(\frac{1}{4}\pi x)\} & (0 \leqslant x \leqslant 4), \\ D & (4 \leqslant x \leqslant L-4), \\ 1+\frac{1}{2}(D-1)\{1-\cos(\frac{1}{4}\pi(L-x))\} & (L-4 \leqslant x \leqslant L). \end{cases} \tag{4.1}$$

The expansion ratio of the channel is D and in all cases the expansion occurs over the length $0 < x < 4$. It can be seen that the transformation from (x, z) to (x, y) coordinates is not orthogonal, so we expect errors in the finite-difference scheme to become large as D becomes large.

We define a norm-like state variable ζ to measure the asymmetry of the flow, where

$$\zeta^2 = \frac{\int_0^L \mathrm{d}x \int_{-f(x)}^{f(x)} \mathrm{d}z\{\psi(x,z)+\psi(x,-z)\}^2}{\int_0^L \mathrm{d}x \int_{-f(x)}^{f(x)} \mathrm{d}z}, \tag{4.2}$$

$\zeta > 0$ if the mainstream is deflected towards the upper wall and $\zeta < 0$ if it is directed towards the lower wall. The flow is symmetric about the centreline $z = 0$, i.e. ψ is an odd function of z, if and only if $\zeta = 0$. We envisage the solution ψ as a point in an infinite-dimensional space which varies as R is increased, and ζ as a map of the solution, for each value of R, into the (R, ζ)-plane. Note also that the single state variable ζ does not completely characterize the flow; only the stream function ψ does that. Consequently there are instances below in which ambiguity arises when we follow the development of the solution as R varies. The first channel we studied was for $L = 80$ and $D = 3$. It is known from laboratory experiments that flow through a channel with a 3:1 expansion ratio becomes asymmetric when $R \approx 20$. For this configuration separation arises when $R \approx 5$. We show in figure 4 the streamlines of symmetric and asymmetric steady flows as R varies. When we calculate ζ (see figure 5), we find that the first bifurcation occurs at $R_c = 5.95$. We have shown that this

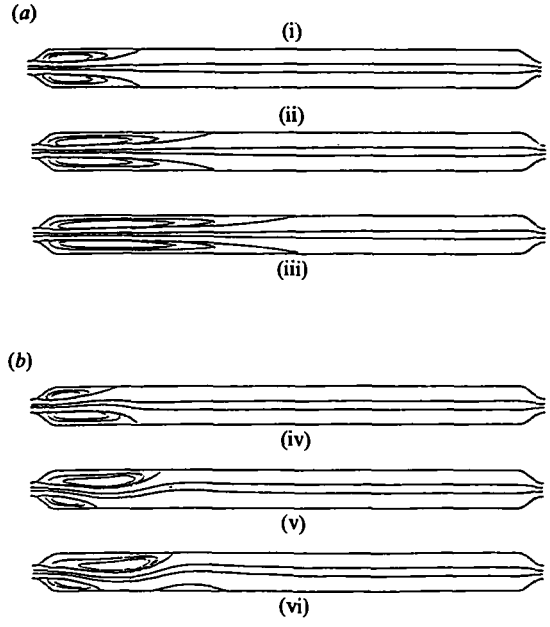

FIGURE 4. Calculated streamlines for both symmetric and asymmetric steady flow through a channel with $D = 3$ and $L = 80$. (*a*) Symmetric flows (i) $R = 30$, (ii) $R = 50$, (iii) $R = 75$. (*b*) Asymmetric flows (iv) $R = 30$, (v) $R = 50$, (vi) $R = 75$.

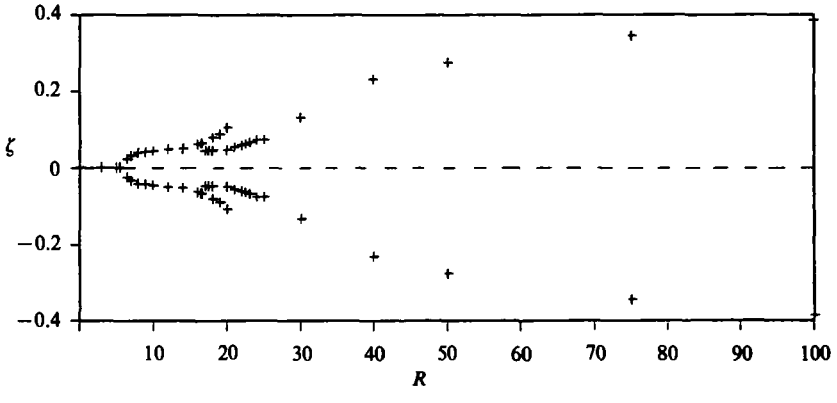

FIGURE 5. Calculated bifurcation diagram for a channel with $D = 3$ and $L = 80$.

is a pitchfork by plotting ζ^2 against R and confirming plausibly that the stream functions of the two asymmetric steady flows are of the form

$$\psi_{\pm}(x, z, R) = \Psi(x, z, R_c) \pm (R - R_c)^{\frac{1}{2}} \hat{\psi}_1(x, z, R_c) + O(R - R_c) \quad \text{as } R \to R_c^+, \quad (4.3)$$

where Ψ is the stream function of the symmetric flow and $\hat{\psi}_1$ is the antisymmetric most unstable eigenfunction. In particular, we calculated the most unstable symmetric solution Ψ and a stable asymmetric solution ψ_+ for $R > R_c$, and hence estimated ψ_- as $2\Psi - \psi_+$; the estimation was confirmed when R was close to R_c by taking the estimate as the initial solution in a subsequent initial-value calculation. In this manner the existence of both ψ_+ and ψ_- was confirmed, i.e. there are two steady stable solutions when $R - R_c$ is small and positive. As R is increased the asymmetry

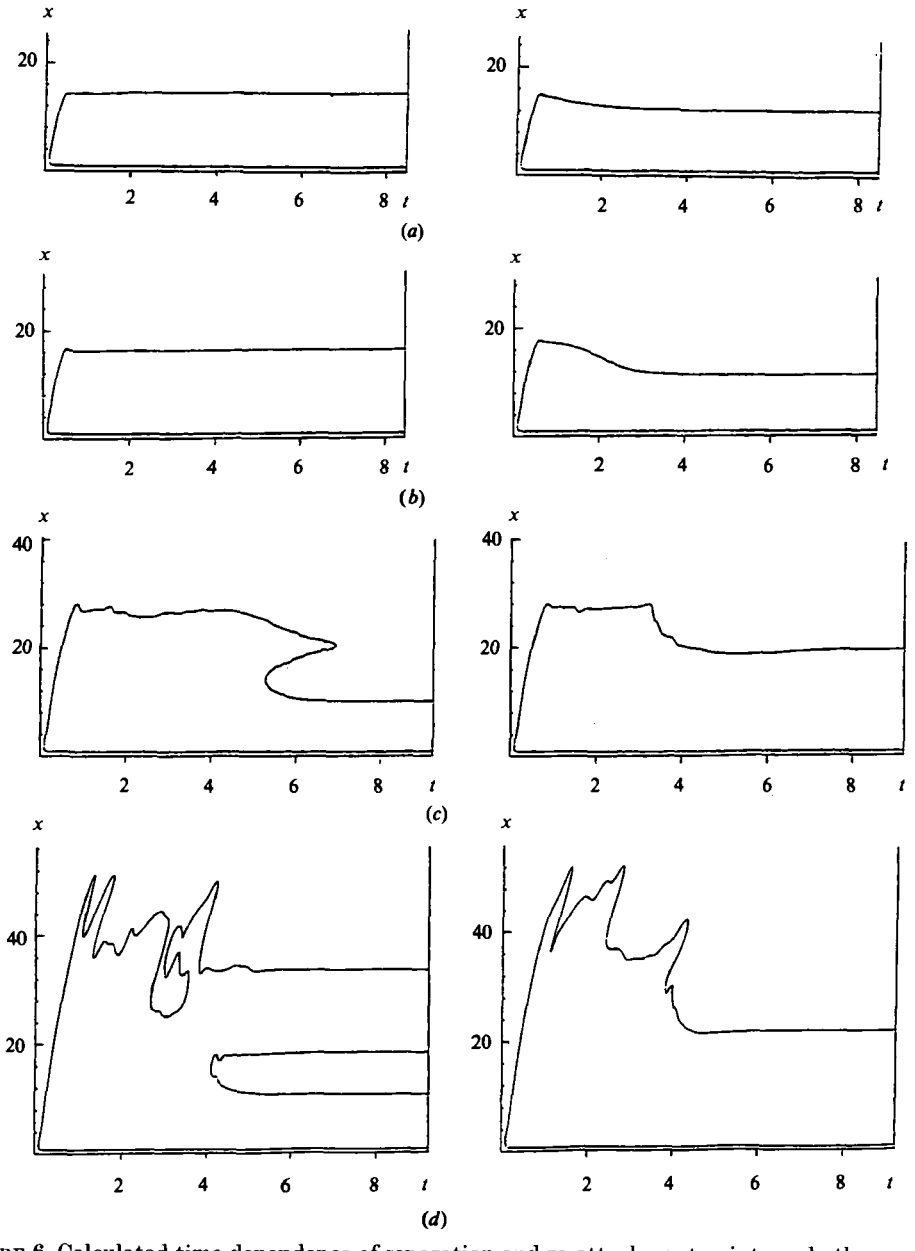

FIGURE 6. Calculated time dependence of separation and re-attachment points on both upper (left side) and lower (right side) walls of a channel with $D = 3$ and $L = 80$. (*a*) $R = 25$, (*b*) $R = 30$, (*c*) $R = 50$, (*d*) $R = 100$.

increases until another bifurcation occurs and a new stable solution appears. By decreasing R afterwards, we found that over the range $15 < R < 20$ there were four stable solutions. This behaviour seems to be due to two simple turning points connecting a branch of unstable steady solutions (which we have not calculated) with the two branches of stable steady solutions found, but may be related to a secondary instability of the symmetric flow to asymmetric disturbances. However, when $D = 1$ and there is plane Poiseuille flow, it is well-known that there is no secondary

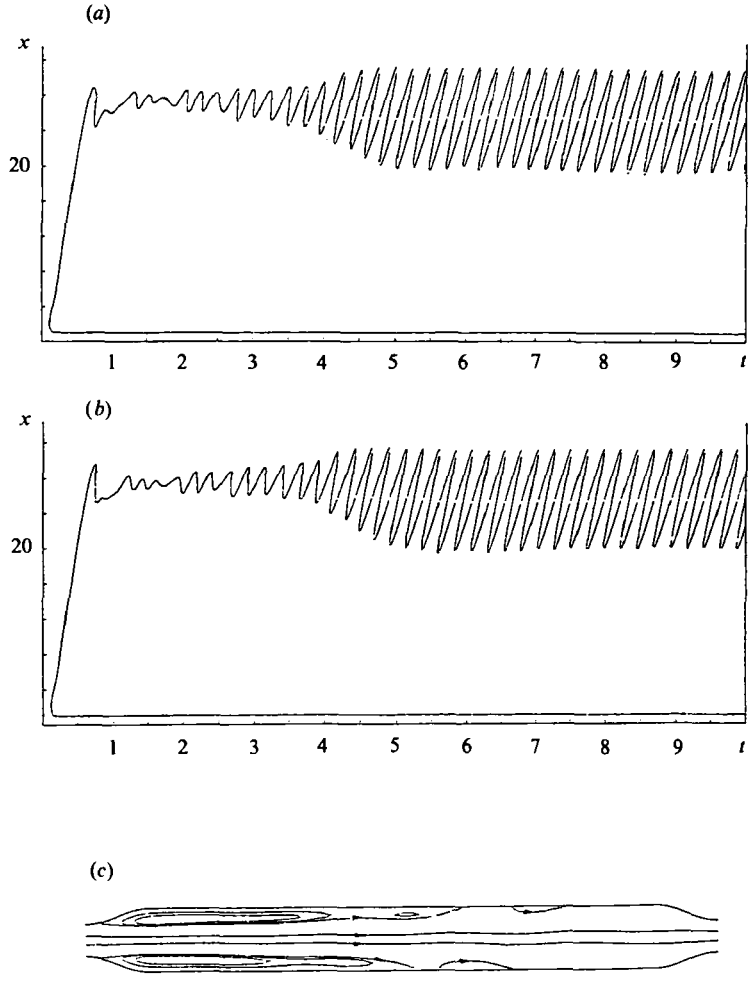

FIGURE 7. Time development of oscillatory solutions in a channel with $D = 2$ and $L = 40$ when $R = 165$. (*a*) Upper wall, (*b*) lower wall, (*c*) instantaneous streamlines.

instability, and indeed, the primary instability follows a Hopf bifurcation. For $R > 30$ we found only two stable solutions. There is little asymmetry for $R < 30$. Recalling that the stream function ψ varies between ± 1, we see that the values of ζ in this range of R represent asymmetries of a few per cent of the variation of ψ. For $R > 30$ the asymmetry becomes much larger, and it is this that has been observed by Cherdron *et al.* (1978) in their laboratory experiments. The first bifurcation has not yet been observed.

Another way of describing the flow is to plot the development in time of the position of the vortices, or separation bubbles, near the walls, as in figure 6. It can be seen that even though the solution is globally stable there are what appear to be small local instabilities of the shear layers in the downstream vicinity of the separation points. These disturbances grow as R increases to about 20 and thereafter *decrease*, disappearing when R approaches 100.

The channel length 80 was studied first because we wished to minimize the effect of the finiteness of the channel length. Such a long channel requires very large computational effort, so we reduced the length of the channel to 40 in order to study

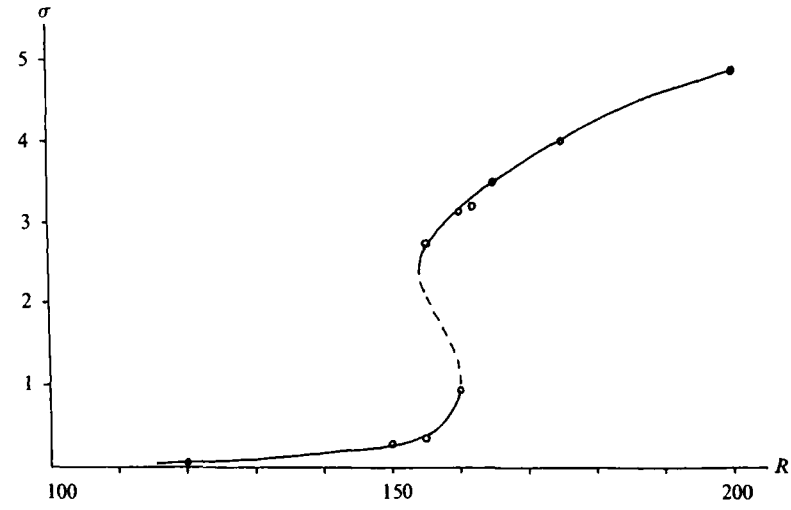

FIGURE 8. Variation of the state variable 'standard deviation of the position of the re-attachment point against time' versus Reynolds number for a channel with $D = 2$ and $L = 40$.

systematically the effect of varying the expansion ratio. Comparison of results for $L = 40$ and $L = 80$ at $D = 2$ suggests that they are qualitatively similar and that the point of bifurcation does not depend sensitively on large L. If $D = 2$ and $L = 40$ then for $R < 11$ there is a unique steady solution which is stable and symmetric. For higher values of R a pitchfork bifurcation occurs and there are two stable asymmetric steady solutions, and one unstable symmetric steady solution. As R increases further there is a turning point and then four stable asymmetric steady solutions, and by inference, three unstable steady solutions, one of which is the only symmetric solution; we do not find large asymmetries in the range $R < 100$, rather the asymmetric solutions are very close to being symmetric. As R increases to near 100 the flow becomes unsteady, the re-attachment point oscillating. This agrees with descriptions of observations which have been presented in the literature. We deduce that a Hopf bifurcation occurs, although we have not been able to calculate the bifurcation point accurately. When R increases to about 150 the periodicity of the solution is clear; in figure 7 we show both the instantaneous streamlines, and graphs of the separation and re-attachment points as functions of time. It can be seen that the vortices are shed from the main vortices behind the expansion and that it is this shedding process which is periodic. We have defined a state variable to describe the periodic solutions by calculating the standard deviation of the re-attachment point as it oscillates. In figure 8 we show the variation of this variable with R. It can be seen that there is a new bifurcation with two stable periodic solutions for a small range of R.

We have calculated the bifurcation diagram for $1.25 \leqslant D \leqslant 2.5$ and $R < 100$, as shown in figure 9. At larger values of D, for example $D = 2.5$, the bifurcation diagram corresponds to the description above for $L = 80$. A pitchfork bifurcation occurs at a low value of R and there are two stable solutions and one unstable solution. Then there are four stable solutions so that hysteresis may occur; by inference, there are three unstable solutions. Thereafter two stable asymmetric solutions remain. As the expansion ratio decreases the picture changes. Firstly we did not find large asymmetry at large values of R. Secondly the region of hysteresis becomes more complicated and more stable solutions arise. For a channel with $L = 40$, $D = 1.35$ and $R = 80$, we found four stable solutions with $\zeta > 0$ and infer that there are seven

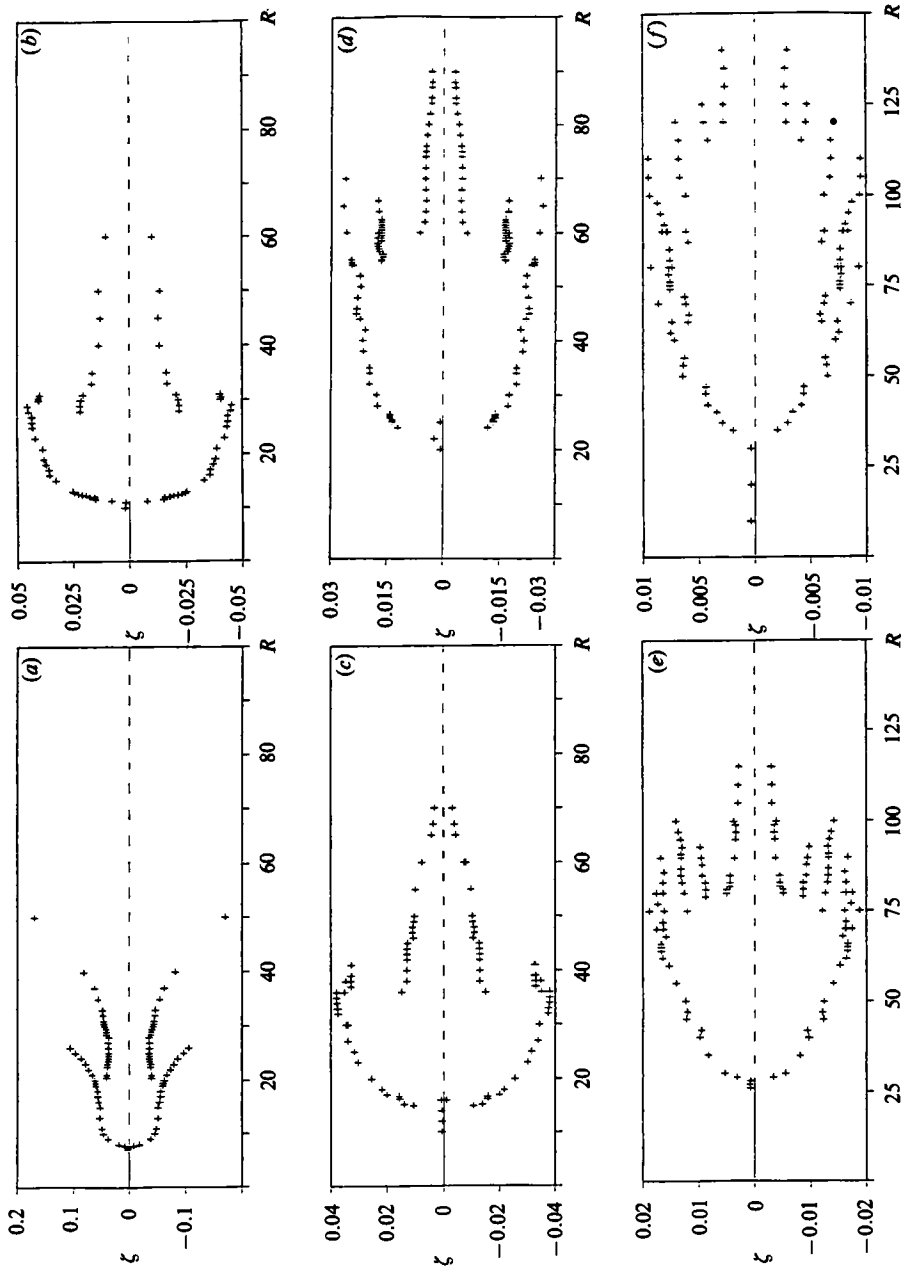

FIGURE 9. Calculated values of the state variable ζ as the Reynolds number varies for $L = 40$, (*a*) $D = 2.5$, (*b*) $D = 2.0$, (*c*) $D = 1.75$, (*d*) $D = 1.5$, (*e*) $D = 1.35$, (*f*) $D = 1.25$. Note that the values of $\zeta < 0$ are inferred from the values of $\zeta > 0$.

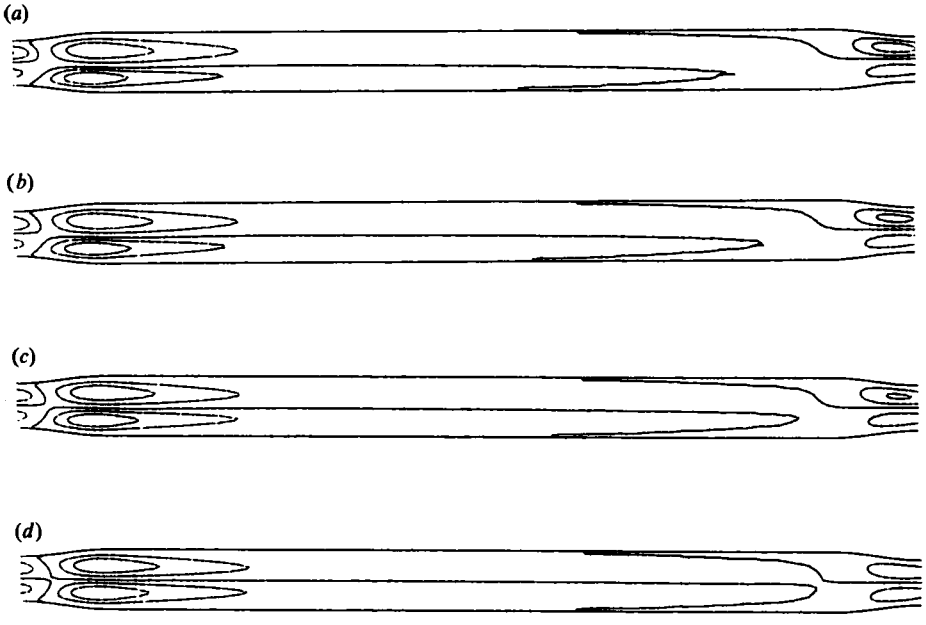

FIGURE 10. Perturbation streamlines of four stable solutions found for $L = 40$ and $D = 1.35$ at $R = 80$. By inference four other stable solutions exist and seven unstable solutions. The stable solutions are obtained by reflecting these streamlines about the centreline of the channel.

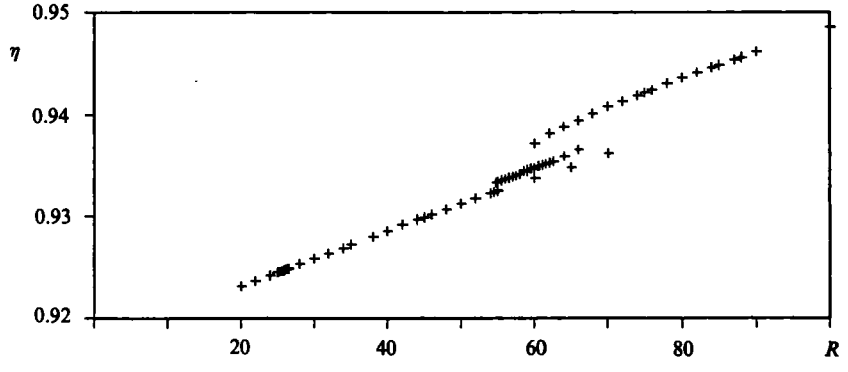

FIGURE 11. Calculated values of the variable η as the Reynolds number varies for a channel with $L = 40$ and $D = 1.5$. Cf. figure 9(*d*).

unstable and eight stable steady solutions in this case. The stream functions of the four stable solutions with $\zeta > 0$ are indicated in figure 10, where we have contoured $\psi - \frac{1}{2}(3y - y^3)$, the difference between the calculated stream function and the stream function of the local plane Poiseuille flow. As D is decreased there is much scatter in the bifurcation diagram. It is difficult to determine the cause of this while we are using only one functional of the stream function. So we calculated a second state variable, η, for the case $D = 1.5$, defining it by

$$\eta^2 = \frac{\int_0^L \mathrm{d}x \int_{-f(x)}^{f(x)} \mathrm{d}z \{\psi(x,z) - \psi(x,-z)\}^2}{\int_0^L \mathrm{d}x \int_{-f(x)}^{f(x)} \mathrm{d}z}, \tag{4.4}$$

where $\eta \geqslant 0$. In figure 11 we plot the calculated values of η against R. The scatter disappears and the different solution branches are clearly visible. Thus the scatter seems to be an artefact of our use of a single state variable ζ to represent the stream function. Note also that the magnitude ζ of the asymmetry decreases as the expansion ratio D decreases.

These basic results will be interpreted below. The computations are lengthy and expensive in terms of CPU time, figures 8 to 15 representing 30 h of CPU time of a CRAY computer. Only a limited amount of information can be communicated effectively, so we have characterized the flows by the state variables η and ζ, the positions of the points of separation and re-attachment, and the contours of the stream function.

5. Results of laboratory experiments

We have described many flows above, calling some of them stable and others unstable. In calling a flow stable we have usually assumed the implicit qualification that it is stable to two-dimensional disturbances, because our methods are restricted to those disturbances. It is important then to find whether the flows we have described as stable are indeed stable to three-dimensional disturbances. The evidence for this must at this stage come from laboratory experiments. The large literature on experimental observations of channel flows is invaluable here. Also we have observed the flow of water through channels by illuminating small reflective particles suspended in the water. Two symmetric 'two-dimensional' channels were used. In one a 15×1 mm rectangular section undergoes a right-angled expansion to a 15×3 mm section. In the other a 15×3 mm section contracts smoothly to a 15×1 mm section and then expands smoothly to the original channel size. Of course, all flows in these channels, with finite width, were three-dimensional. In both channels the general sequence of events as R increased was first steady flows symmetric in both transverse directions, then steady flows asymmetric in the 'plane' of the flow but symmetric in the perpendicular direction, i.e. across the flow, and finally unsteady flows. We could not observe the unsteady flows closely enough to be sure, but our impression is that means of the unsteady flows are symmetric across the channel and asymmetric in the plane of the flow. Sobey (1985) has illustrated this sequence in the case of a sudden channel expansion. To demonstrate the importance of the nature of the expansion we show here photographs taken in a channel which contracts and expands smoothly. In figures 12 (a, b) when $R = 40$ the flow is symmetric in both the plane of the flow and across the channel. Figure 12 (b) should be contrasted with figure 2 (f) in Sobey (1985). At higher Reynolds numbers, in this case $R = 85$, the flow is asymmetric in the plane of the flow but still symmetric across the channel (figure 12 c, d).

Other points come from the literature. For a 3:1 expansion ratio, the value of the Reynolds number at which asymmetries have been first observed is from 20 to 30 according to the aspect ratio of the channel. It can be seen from figure 5 that this agrees with our calculation that *large* asymmetries occur for $R > 30$. We predict small asymmetries for the range $R < 30$ which appear not to have been observed yet, but laser-Doppler techniques may provide a means of observing them.

Cherdron *et al.* (1978) reported oscillations in the neighbourhood of the re-attachment point, and they found small oscillations near the separation point. It is important to distinguish between oscillations near the separation point, which may be no more than a symptom of a small local instability in an otherwise steady flow,

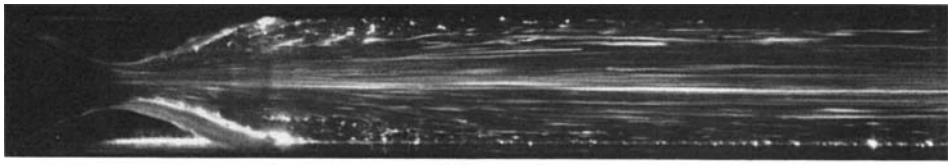

(*a*)

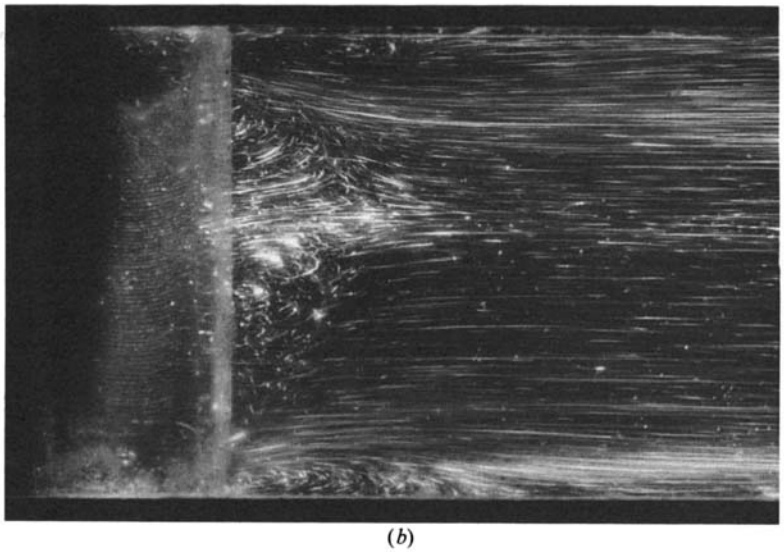

(*b*)

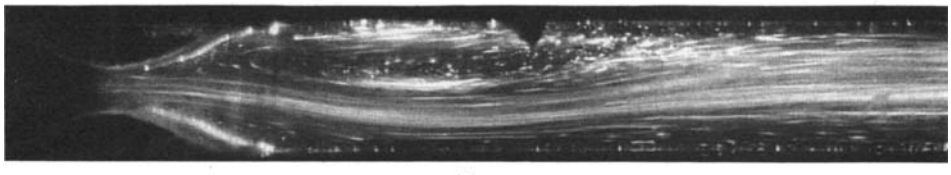

(*c*)

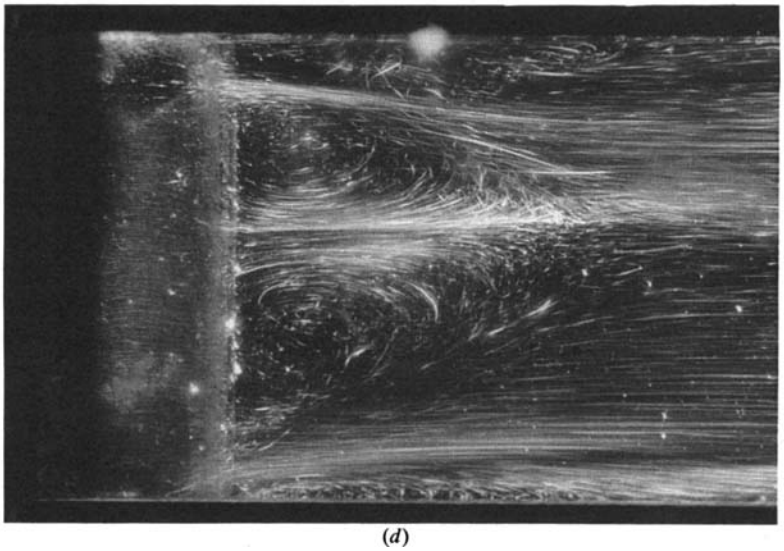

(*d*)

FIGURE 12. Observation of flow in a channel showing three-dimensionality of the flow field. (*a*) $R = 40$, centreplane illuminated, (*b*) $R = 40$, viewed from above, (*c*) $R = 85$, centreplane illuminated, (*d*) $R = 85$, viewed from above.

D	1.25	1.35	1.5	2	2.5	3
R_c	32	27	21	11	8	6
R_{JH}	47	34	25	12	8.9	5.8
R_{sep}	215	94	40	12	7	5

TABLE 2. Values, as D varies, of (i) the critical value R_c of the Reynolds number calculated for the primary bifurcation of channel flows with $L = 80$, (ii) the critical value R_{JH} of the Reynolds number for the bifurcation $\mathscr{B}_2$ of Jeffery–Hamel flows (based on table 1 and the maximum angle of slope of the channel wall), and (iii) the Reynolds number R_{sep} calculated at the onset of separation in channel flows with $L = 80$ (note that the values for D close to one are uncertain because of the numerical errors at large values of R)

and oscillations near the re-attachment point, which are a better indication that the flow has become globally unsteady.

6. Conclusions

We have introduced bifurcation theory and applied it in detail to two examples of two-dimensional flows, Jeffery–Hamel (JH) flows and numerical solutions for channel flows. Here we first discuss the relationship of JH to channel flow. If JH flows were to be local approximations to flow through a slowly varying channel then we would expect the breakdown of symmetric JH flow to correspond to the first bifurcation observed in the numerical solutions for channel flow. The evidence we have given above does not support this correspondence because the qualitative nature of the symmetry breaking differs in the two examples. For JH flows there is a *sub*critical pitchfork bifurcation and no stable flow above a certain value either of the Reynolds number (for a fixed configuration of the channel), or the maximum angle between the channel walls (for a fixed value of the Reynolds number). For channel flows, our calculations show a *super*critical pitchfork bifurcation and stable steady asymmetric flows for much higher values of the Reynolds number.

It is remarkable that channel flows have a supercritical bifurcation although JH flows both have a subcritical bifurcation and approximate wall channel flows upstream of the station x where the angle $\alpha = \tan^{-1}(\mathrm{d}f/\mathrm{d}x)$ is a maximum. In any event, it seems that JH flows are irrelevant to a channel flow downstream of a point of separation. It is also remarkable that the correlation between the JH estimate of the station of both bifurcation and separation in table 2 is worst when D is closest to one, i.e. when

$$\frac{\mathrm{d}\alpha}{\mathrm{d}x} = \frac{\mathrm{d}^2 f}{\mathrm{d}x^2} \Big/ \left\{1 + \left(\frac{\mathrm{d}f}{\mathrm{d}x}\right)^2\right\}$$

is least. Perhaps a more effective measure of the rapidity of the change of α than $\mathrm{d}\alpha/\mathrm{d}x$ is

$$\frac{\mathrm{d}\alpha}{\mathrm{d}z} = \frac{\mathrm{d}\alpha}{\mathrm{d}x} \Big/ \frac{\mathrm{d}f}{\mathrm{d}x}.$$

However it is more rational to infer that the approximation of the slow variation of α is valid when $\lambda\, \mathrm{d}\alpha/\mathrm{d}x \ll 1$, where λ is the total lengthscale of decay downstream of the least stable normal mode of the linearized steady problem. Wilson (1969) used this method to examine the spatial adjustment of steady flows to plane Poiseuille flow successfully, although the definition of λ is not so clear for non-parallel flows.

Then we would expect λ to be small where the channel flow is locally very stable, i.e. near the entrance, and become infinite where there is local instability, i.e. in the throat when $R > R_c$. This argument indicates that JH flows are good local approximations to a channel flow where it is locally stable, but does not explain why the approximation is worst when $D \approx 1$.

Symmetric JH flows do approximate channel flows near the inlet, and give a useful estimate of the value R_c of the Reynolds number at which channel flows first bifurcate, as table 2 shows for various values of D. Further separation occurs near the station where the slope of the channel is greatest. Table 2 also shows that as D decreases towards one the JH approximation worsens, channel flows becoming unstable to asymmetric disturbances before JH flow based on the maximum wall slope does. Although it must be remembered that JH flows are strictly comparable to channel flows only if the angle between the channel walls changes very slowly downstream and that we used channels with angles which do not change slowly, we believe that the discrepancies noted above are of deeper significance.

Separation and bifurcation are conceptually different phenomena, but are sometimes confused because they may appear to arise together. Separation is the reversal of flow near a wall. Bifurcation is a change in the number of flows which may occur in a given configuration at a given value of the Reynolds number. We have shown that for symmetric channels there is a unique steady symmetric flow when $R < R_c$ which becomes unstable as R passes through R_c, the first eigenfunction, $\hat{\psi}_1$, being in general antisymmetric at the onset of instability. Weakly nonlinear theory gives formula (4.3) to describe the two asymmetric steady flows for small positive values of $R - R_c$. If Ψ_{nn}, the normal gradient of the tangential velocity, vanishes at a wall when $R = R_c$ then the second term on the right-hand side of (4.3) dominates the first term sufficiently close to the wall, however small $R - R_c$ may be. Therefore there is separation near the wall. Now for JH flows, $\Psi_{nn} = 0$ at the walls when $R = R_c$ so separation and bifurcation arise together. For plane Poiseuille flow, $\Psi_{nn} \neq 0$ at the walls when $R = R_c$ and the primary bifurcation is a Hopf, not a pitchfork, so separation and bifurcation do not arise together. Table 2 shows that for channel flows separation and bifurcation in general do not arise together.

Many of our numerical results follow those of Cliffe & Greenfield (1982), who considered flows through a two-dimensional channel with an expansion but no contraction. Not only are the shape of their expansion and their boundary conditions different from ours, but they solved only steady problems by the Newton–Raphson method for an expansion ratio 2:1. The advantage of the Newton–Raphson method is that it may converge clearly to unstable as well as stable steady solutions, but it does not give the evolution of flows as time increases. In any event, using the distance downstream of the point of re-attachment on the upper wall as a state variable and a Reynolds number as the control variable, they showed clearly that there is symmetry breaking at a pitchfork bifurcation. They found the bifurcation at much higher values of the Reynolds number than we have done, and that may be because the boundary conditions we have applied are periodic in the direction of flow whilst theirs were not, or because the shape of their channel differs from ours. We have seen that the maximum angle of the channel throat is an important factor in determining the critical value of the Reynolds number.

Further our numerical results connect plane Poiseuille flow with more general channel flows. For values of $D \approx 3$, we have calculated steady asymmetric flows for which the degree of asymmetry is large. At values of $D \approx 2$, we find steady solutions with a small degree of asymmetry and at large values of the Reynolds number,

unsteady solutions. As the expansion ratio approaches one we have found only small steady asymmetries. In the limit as $D \to 1$ there is only a subcritical Hopf bifurcation of plane Poiseuille flow.

In order to establish the connection between these flows we must first return to the nature of our solutions. Our calculations are imperfect; numbers are stored with finite accuracy, the differential equations which describe the flow are represented by a nonlinear set of difference equations which are solved with a finite accuracy. The difference equations are known to model the differential equations with a great degree of similitude for small values of the Reynolds number. At larger values of R the correspondence between the differential equations and the difference equations decreases. When several different stable solutions exist each will have a domain of attraction in the multi-dimensional space for which the stream function is but a point. The fine details of the numerical scheme and the manner in which numbers are represented by a finite number of digits will place any initial value of the stream function in the domain of attraction of a particular solution. The finiteness of the time for which the calculation proceeds may mean that the stream function may not have reached the close vicinity of the stable solution when the calculation is stopped. These ideas all indicate that numerical solutions should be approached with a certain degree of scepticism unless they are supported by experimental evidence.

Our interpretation of the results is then as follows. At large values of D the bifurcation to steady asymmetric flow produces a very stable flow structure, and one for which we have not been able to calculate time-periodic two-dimensional solutions. As D decreases the steady asymmetric solutions are less stable (in the sense that their domain of attraction in the stream function space is smaller) and for $R \lesssim 100$ we calculate steady solutions and for $R \gtrsim 100$ we calculate time-periodic solutions. We have not been able to track the steady asymmetric solutions in this region, and the limited accuracy of our calculations has made it impossible to identify precisely the onset of time-periodic solutions. As D approaches one the magnitude of the steady asymmetry decreases and the value of R for the first bifurcation rises rapidly. For these flows we were not able to calculate any time-periodic solutions, presumably because the point of bifurcation to time-periodic solutions occurs at much larger R; nevertheless it is plausible that it is in this way that the Hopf bifurcation at $D = 1$ is achieved.

Experiments have realized some of the stable asymmetric flows described by our two-dimensional calculations. Some of the asymmetries we have presented are well known, others are new. We hope that further experiments will confirm the rich structure which our numerical calculations have demonstrated.

We are grateful to Professor L. E. Fraenkel for discussion of Jeffery–Hamel flows.

REFERENCES

BENJAMIN, T. B. 1978 *Proc. R. Soc. Lond.* A **359**, 1.

BUITRAGO, S. E. 1983 M. Phil. thesis, University of Sussex.

CHERDRON, W., DURST, F. & WHITELAW, J. H. 1978 *J. Fluid Mech.* **84**, 13.

CLIFFE, K. A. & GREENFIELD, A. C. 1982 *Report* TP 939 AERE, Harwell.

DAVIS, S. H. 1969 *Proc. R. Soc. Lond.* A **310**, 341.

DIPRIMA, R. C. & HALL, P. 1984 *Proc. R. Soc. Lond.* A **396**, 75.

DRAZIN, P. G. 1961 *J. Fluid Mech.* **10**, 571.

DRAZIN, P. G. & REID, W. H. 1981 *Hydrodynamic Stability*. Cambridge University Press.
EAGLES, P. M. 1966 *J. Fluid Mech.* **24**, 191.
EAGLES, P. M. 1973 *J. Fluid Mech.* **57**, 149.
EAGLES, P. M. & SMITH, F. T. 1980 *J. Engng Maths* **14**, 219.
EAGLES, P. M. & WEISSMAN, M. A. 1975 *J. Fluid Mech.* **69**, 241.
FRAENKEL, L. E. 1962 *Proc. R. Soc. Lond.* A **267**, 119.
FRAENKEL, L. E. 1963 *Proc. R. Soc. Lond.* A **272**, 406.
FRAENKEL, L. E. 1973 *Proc. Camb. Phil. Soc.* **73**, 61.
GEORGIOU, G. A. & EAGLES, P. M. 1985 *J. Fluid Mech.* **159**, 259.
GILLANI, N. V. & SWANSON, W. M. 1976 *J. Fluid Mech.* **78**, 99.
HAMEL, G. 1916 *Jahresbericht der Deutschen Math. Vereinigung.* **25**, 34.
HOOPER, A., DUFFY, B. R. & MOFFATT, H. K. 1982 *J. Fluid Mech.* **117**, 283.
JEFFERY, G. B. 1915 *Phil. Mag.* **29** (6), 455.
MOFFATT, H. K. & DUFFY, B. R. 1980 *J. Fluid Mech.* **96**, 299.
SERRIN, J. 1959 *Handbuch der Physik* **8**(1), 253.
SOBEY, I. J. 1980 *J. Fluid Mech.* **96**, 1.
SOBEY, I. J. 1982 *J. Fluid Mech.* **125**, 359.
SOBEY, I. J. 1985 *J. Fluid Mech.* **151**, 395.
WILLE, R. & FERNHOLZ, H. 1965 *J. Fluid Mech.* **23**, 801.
WILSON, S. 1969 *J. Fluid Mech.* **38**, 793.
WOODS, L. C. 1954 *Aero. Quart.* **5**, 176.